

# **Separations and Waste Forms Campaign: Equilibrium Temperature Profiles within Fission Product Waste Forms**

---

**Nuclear Engineering Division**

### **About Argonne National Laboratory**

Argonne is a U.S. Department of Energy laboratory managed by UChicago Argonne, LLC under contract DE-AC02-06CH11357. The Laboratory's main facility is outside Chicago, at 9700 South Cass Avenue, Argonne, Illinois 60439. For information about Argonne and its pioneering science and technology programs, see [www.anl.gov](http://www.anl.gov).

### **DOCUMENT AVAILABILITY**

**Online Access:** U.S. Department of Energy (DOE) reports produced after 1991 and a growing number of pre-1991 documents are available free via DOE's SciTech Connect (<http://www.osti.gov/scitech/>)

**Reports not in digital format may be purchased by the public from the National Technical Information Service (NTIS):**

U.S. Department of Commerce  
National Technical Information Service  
5301 Shawnee Rd  
Alexandria, VA 22312  
**[www.ntis.gov](http://www.ntis.gov)**  
Phone: (800) 553-NTIS (6847) or (703)  
605-6000 Fax: (703) 605-6900  
Email: [orders@ntis.gov](mailto:orders@ntis.gov)

**Reports not in digital format are available to DOE and DOE contractors from the Office of Scientific and Technical Information (OSTI):**

U.S. Department of Energy  
Office of Scientific and Technical Information  
P.O. Box 62  
Oak Ridge, TN 37831-0062  
**[www.osti.gov](http://www.osti.gov)**  
Phone: (865) 576-8401  
Fax: (865) 576-5728  
Email: [reports@osti.gov](mailto:reports@osti.gov)

### **Disclaimer**

This report was prepared as an account of work sponsored by an agency of the United States Government. Neither the United States Government nor any agency thereof, nor UChicago Argonne, LLC, nor any of their employees or officers, makes any warranty, express or implied, or assumes any legal liability or responsibility for the accuracy, completeness, or usefulness of any information, apparatus, product, or process disclosed, or represents that its use would not infringe privately owned rights. Reference herein to any specific commercial product, process, or service by trade name, trademark, manufacturer, or otherwise, does not necessarily constitute or imply its endorsement, recommendation, or favoring by the United States Government or any agency thereof. The views and opinions of document authors expressed herein do not necessarily state or reflect those of the United States Government or any agency thereof, Argonne National Laboratory, or UChicago Argonne, LLC.

# **Separations and Waste Forms Campaign: Equilibrium Temperature Profiles within Fission Product Waste Forms**

---

by  
Michael D. Kaminski  
Nuclear Engineering Division, Argonne National Laboratory

October 2016



## CONTENTS

<b>Summary.....</b>	<b>1</b>
<b>1 Introduction.....</b>	<b>3</b>
<b>2 Methods.....</b>	<b>4</b>
<b>3 Results and Discussion.....</b>	<b>10</b>
3.1 Equilibrium Centerline Temperatures for Benchmark Glasses .....	10
3.2 $\gamma$ -Ray Absorption .....	14
3.3 Effect of Cracking.....	15
3.4 Coolant Heating along Vertical Elements.....	17
3.5 Active Cooling of Waste Forms in Air and Passive Cooling in Water .....	17
3.6 Equilibrium Temperature for Buried Waste Forms .....	18
<b>4 Conclusions.....</b>	<b>20</b>
<b>Acknowledgments .....</b>	<b>22</b>
<b>References .....</b>	<b>23</b>
<b>Appendix A Summary Data for Waste Forms .....</b>	<b>24</b>

## FIGURES

1	Specific power of Cs-134, Cs-137, and total cesium a function of fraction of $\gamma$ -rays deposited within a canister. ....	8
2	Waste form diameter and required number of 4.6-m long canisters per 1000 MTHM processed per year for three candidate waste glass compositions as a function of the cooling period prior to processing fuel.....	10
3	Centerline temperature for different diameter glasses for the three baseline waste glass compositions. ....	11
4	Relationship between the equilibrium centerline temperature and the power produced within a canister. ....	12
5	Aggregate of equilibrium centerline temperature data for the three waste form glasses for $T_{\text{centerline}} \leq 800^{\circ}\text{C}$ . Line fit of data is for second-order polynomial.....	13
6	Equilibrium centerline temperature of CSLNTM-C-2.5, assuming increasing value for fraction of $\gamma$ -rays absorbed within the waste form. ....	14

## FIGURES (CONT.)

7	Equilibrium centerline temperatures as function of thermal conductivity $k$ .....	16
8	Centerline temperature as a function of thermal conductivity for the three baseline waste glasses with cracks. Cracks were modeled as fractional porosity from 0.08 to 0.3. ....	16

## TABLES

1	Compositions of baseline lanthanide borosilicate glasses evaluated in this report. ....	5
2	Lanthanide isotope mass and decay power. ....	6
3	Mass and power from lanthanide fission products. Power is dominated by europium but is still small compared to cesium and strontium decay. ....	6
4	Mass and power from transition metal fission products. ....	7
5	Mass and power values used in the thermal calculations. ....	7
6	Equilibrium centerline temperatures for waste form glasses prepared from 20-y cooled fuel and cooled by air and water. ....	18
7	Equilibrium centerline temperatures for waste form glasses prepared from 20-y cooled fuel and buried in earth.....	18
8	Dilution factors of the waste feed required to produce a 0.610-m diameter waste form with $T_{\text{centerline}} = T_g$ for glasses prepared from 10-, 20-, and 50-y cooled fuel and buried in earth. ....	19
A-1	Data for CSLN-7C at constant $k = 1.0 \text{ W}/(\text{m}\cdot\text{K})$ .....	25
A-2	Data for CSLN-7C as function of $k$ . ....	26
A-3	Data for CSLNTM-C-2.5 at constant $k = 1.0 \text{ W}/(\text{m}\cdot\text{K})$ .....	27
A-4	Data for CSLNTM-C-2.5 as function of $k$ . ....	28
A-5	Data for CSLNTM-B-3.0 at constant $k = 1.0 \text{ W}/(\text{m}\cdot\text{K})$ .....	29
A-6	Data for CSLNTM-B-3.0 as function of $k$ . ....	30

# **SEPARATIONS AND WASTE FORMS CAMPAIGN: EQUILIBRIUM TEMPERATURE PROFILES WITHIN FISSION PRODUCT WASTE FORMS**

## **SUMMARY**

We studied waste form strategies for advanced fuel cycle schemes. Several options were considered for three waste streams with the following fission products: cesium and strontium, transition metals, and lanthanides. These three waste streams may be combined or disposed separately. The decay of several isotopes will generate heat that must be accommodated by the waste form, and this heat will affect the waste loadings. To help make an informed decision on the best option, we present computational data on the equilibrium temperature of glass waste forms containing a combination of these three streams.

The baseline compositions were developed by teams from Pacific Northwest National Laboratory and Savannah River National Laboratory, who noted that two scenarios could limit waste loading into the glass—high molybdenum content and high noble metals content. For the latter scenario, the glass composition identified was borosilicate glass containing a cesium and strontium (CS) stream combined with a lanthanide (LN) stream. For the former scenario, two borosilicate glasses were developed for a CS, LN, and transition metal (TM) fission product stream.

For this effort, we employed a simple computer model that assumes a homogeneously distributed internal heat source with a value calculated from the decay heat of the radionuclides within the waste form (W/g). The iterative model starts by guessing at the value of the total heat transfer coefficient at the outside of a cylindrical waste canister containing the solidified glass product. The model then calculates the temperature profile, and the calculated external wall temperature is used to calculate a revised value for the convective heat transfer coefficient to the coolant fluid. From this, it calculates a new estimate of the total heat transfer coefficient and repeats these operations until the iteration converges.

Our task was to estimate the radial temperature profile within right cylindrical glass monoliths for various waste loadings, radioactive decay power, waste form diameter, and storage/disposal conditions. We evaluated three waste glasses. The first, CSLN-7C, contained only the cesium/strontium stream and the lanthanide elements. The second and third glasses contained these plus the transition metals in different concentrations. The waste loading in CSLNTM-C-2.5 was limited by high  $\text{MoO}_3$ , while the waste loading in CSLNTM-B-3.0 was limited by high noble metals.

The dominant heat source in a waste stream containing the cesium/strontium stream, the lanthanides, and the transition metals is from the decay of Cs-134, Cs-137, Sr-90, and their daughter products Ba-137<sup>m</sup> and Y-90. The maximum diameters for the three baseline glasses ( $k = 1.0$ ) prepared from 20-y cooled fuel were calculated to be:

- 0.278 m (10.94 in.) for CSLN-7C
- 0.470 m (18.5 in.) for CSLNTM-C-2.5
- 0.181 m (14.2in.) for CSLNTM-B-3.0

for centerline temperature equal to the glass transition temperature ( $T_{\text{centerline}}=T_g$ ) under passive cooling in air. For these diameters, the number of canisters required to dispose the waste from 1000 MTHM processed was 67, 92, and 96 for CSLN-7C, CSLNTM-C-2.5, and CSLNTM-B-3.0, respectively. Cooler waste from older fuel (50 y) can be accommodated in larger diameter canisters [0.422 m (16.6 in.), 0.709 m (27.9 in.), and 0.546 m (21.5 in.) for CSLN-7C, CSLNTM-C-2.5, and CSLNTM-B-3.0, respectively], which reduces the number of canisters needed per 1000 MTHM by a factor of three.

We can model the centerline temperature of the baseline glasses as a function of total power within a canister ( $P$ ) by using a simple polynomial fit to the data:

$$T_{\text{centerline}} (^{\circ}\text{C}) = -0.114 \left( P \left[ \frac{kW}{\text{canister}} \right] \right)^2 + 28.9 P \left[ \frac{kW}{\text{canister}} \right] + 139 \quad (R^2 = 0.960).$$

for centerline temperatures  $< \sim 800^{\circ}\text{C}$ . This relationship applies to glass waste forms prepared from 10-, 20-, and 50-y cooled fuel.

We noted the sensitivity of the temperature function to changes in thermal conductivity ( $k$ ) either due to uncertainty in our measurement of the solidified glass or the effects of cracking. For glasses at  $T_{\text{centerline}} = T_g$  prepared from 20-y cooled fuel, the relationship is not linear, with

$$\frac{-dT}{dk}$$

being much larger for  $k < 1 \text{ W}/(\text{m}\cdot\text{K})$  than for  $k > 1 \text{ W}/(\text{m}\cdot\text{K})$ . For  $k = 0.8 \text{ W}/(\text{m}\cdot\text{K})$ ,  $T_{\text{centerline}}$  increases by  $90^{\circ}\text{C}$  for the CSLN-7C waste form (719 to  $807^{\circ}\text{C}$ ) and  $60^{\circ}\text{C}$  for the two CSLNTM waste forms. In contrast, for  $k = 1.2 \text{ W}/(\text{m}\cdot\text{K})$ ,  $T_{\text{centerline}}$  is reduced by  $50^{\circ}\text{C}$  for CSLN-7C (719 to  $660^{\circ}\text{C}$ ) and  $40^{\circ}\text{C}$  for the CSLNTM samples. Experimental data are required for us to properly evaluate the magnitude of cracking and quantify the values of the effective thermal conductivity of the cracked solid.

Finally, we showed that heating of the coolant fluid along a vertically emplaced waste form will result in a  $\Delta T_{\text{centerline}}$  along the z-axis of  $25\text{-}30^{\circ}\text{C}$ . However, active cooling by air will reduce  $T_{\text{centerline}}$  by  $\sim 25\%$ , and passive cooling in water will reduce  $T_{\text{centerline}}$  by  $\sim 40\%$  over the baseline case of passive cooling in air. We also found that burial of fresh waste form glasses will require very low waste loadings to avoid thermal heating to above the glass transition temperature, or they must be cooled for prolonged periods prior to burial.



# 1 INTRODUCTION

For some years now, the U.S. has been developing waste form strategies for advanced fuel cycle schemes [Gombert et al. 2007]. At present, several options are being considered for three waste streams of the following fission products: cesium and strontium, transition metals, and lanthanides. These three waste streams may be combined or disposed separately. The decay of several isotopes will generate heat that must be accommodated by the waste form, and this heat will affect the waste loadings. To help make an informed decision on the best option, we present computational data on the equilibrium temperature of glass waste forms containing a combination of these three streams.

Using a model developed earlier [Kaminski-2005], we calculated the temperature profiles in right cylindrical glass logs containing isotopes separated from pressurized water reactor (PWR) fuel burned to 50 GWd/MT and cooled for 10-50 years. The fission product composition of the glass logs was varied to include (1) cesium and strontium alone and (2) cesium and strontium plus the lanthanides and transition metals. We assumed the glass logs were contained in a baseline 24-in. (0.6-m) diameter, 15-in. (0.4-m) long canister. A baseline waste loading was derived from theoretical and experimental work completed at Pacific Northwest National Laboratory (PNNL) and Savannah River National Laboratory (SRNL) [Crum-2009]. The waste loading and diameter of the canister were varied from the baseline, and the resulting centerline temperature ( $T_{\text{centerline}}$ ) was computed. Then, the canister diameter was varied at the baseline loading to determine the diameter at which the centerline temperature would equal the glass transition temperature ( $T_{\text{centerline}} = T_g$ ). We considered several storage and disposal environments, including passive and active air cooling, passive water cooling, and emplacement in a dehydrated clay barrier. Accompanying these data, we report the number of glass logs required to dispose the waste generated by processing one metric ton of spent fuel and the total thermal power produced within each log.

## 2 METHODS

Baseline waste form compositions were developed by teams from PNNL and SRNL [Crum-2009], who noted that two scenarios could limit waste loading into the glass – high molybdenum content and high noble metals content. Another scenario was chosen for waste glass development because it was not expected to be limited by waste loading. For the latter scenario, the glass composition was the borosilicate glass containing a cesium and strontium (CS) stream combined with a lanthanide (LN) stream (Table 1). For the former scenario, two borosilicate glasses were developed for a CS, LN, and transition metal (TM) fission product stream (Table 1). Experimental data on the physical properties of the baseline glasses were reported [Crum-2009].

For the temperature profile determinations, we employed the computer model developed by Kaminski [2005] with minor upgrades in the algorithms described in the 2007 Advanced Fuel Cycle Initiative (AFCI) quarterly reports. The model algorithm was developed by combining Fourier's heat conduction equations with Newton's law of cooling while modifying key parameters to account for porosity and solid phase mixtures. The model assumes a homogeneously distributed internal heat source  $S_o$  (in W/g glass), which was calculated from the decay heat of the radionuclides within the waste form. The model begins by guessing the value of the total heat transfer coefficient at the outside of a cylindrical waste canister containing the solidified glass product. The model then calculates the temperature profile based on the coefficient, and the calculated external wall temperature is then used to calculate a revised value for the convective heat transfer coefficient to the coolant fluid. Subsequently, the model calculates a new estimate of the total heat transfer coefficient and repeats these operations until the iteration converges.

The composition of selected isotopes in the reference fuel and the decay power were calculated with the ORIGEN code [J. Stillman, personal communication, Argonne National Laboratory] for 10-y and 20-y cooled PWR fuel (4.25% U-235 enrichment, burnup = 50 GWd/MT). We obtained 50-y cooled data by applying a 30-y decay period to each radioisotope from the data set for the 20-y cooled fuel, using

$$A(t = 50 \text{ y}) = A(t = 20 \text{ y})e^{-\lambda t_{30}}, \quad (1)$$

where  $t_{30} = 30 \text{ y}$ , and  $\lambda$  is the decay constant for that particular radionuclide. Because lanthanide and transition metal isotopes have low specific power and/or low abundance, they do not represent a significant heat source and were thus ignored. Tables 2-4 present the mass and power per metric ton heavy metal (HTHM) for the lanthanide isotopes, the lanthanide fission products, and the transition metal fission products, respectively.

**TABLE 1 Compositions (in mass%) of baseline lanthanide borosilicate glasses evaluated in this report (data from [Crum-2009]).**

Oxide	CSLN-7C (CS+LN <sup>a</sup> )	CSLNTM-C-2.5 (High MoO <sub>3</sub> +CS+LN+TM <sup>b</sup> )	CSLNTM-B-3.0 (High Noble Metals CS+LN+TM <sup>c</sup> )
Ag <sub>2</sub> O	-	0.07	0.11
Al <sub>2</sub> O <sub>3</sub>	17.0	5.95	6.53
B <sub>2</sub> O <sub>3</sub>	10.0	5.00	5.16
BaO	5.71	1.41	2.2
CaO	-	7.00	5.16
CdO	-	0.07	0.11
CeO <sub>2</sub>	7.04	1.98	3.09
Cs <sub>2</sub> O	5.98 <sup>d</sup>	1.84 <sup>e</sup>	2.87 <sup>f</sup>
Eu <sub>2</sub> O <sub>3</sub>	0.41	0.11	0.17
Gd <sub>2</sub> O <sub>3</sub>	0.46	0.1	0.16
La <sub>2</sub> O <sub>3</sub>	3.59	1.01	1.58
Li <sub>2</sub> O	-	4.02	3.21
MoO <sub>3</sub>	-	2.50	0.78
Na <sub>2</sub> O	-	7.00	7.22
Nd <sub>2</sub> O <sub>3</sub>	11.86	3.36	5.22
PdO	-	0.01	0.02
Pr <sub>2</sub> O <sub>3</sub>	3.28	0.93	1.44
Rb <sub>2</sub> O	0.77	0.27	0.42
RhO <sub>2</sub>	-	0.05	0.07
RuO <sub>2</sub>	-	0.13	0.18
SeO <sub>2</sub>	-	0.05	0.08
SiO <sub>2</sub>	28.0	53.03	49.94
Sm <sub>2</sub> O <sub>3</sub>	2.49	0.69	1.07
SnO <sub>2</sub>	-	0.04	0.07
SrO	1.98 <sup>d</sup>	0.63 <sup>e</sup>	0.98 <sup>f</sup>
TeO <sub>2</sub>	-	0.42	0.65
Y <sub>2</sub> O <sub>3</sub>	1.43	0.40	0.63
ZrO <sub>2</sub>	-	1.91	0.87
Total	100	100	100
Density	3.36 g/cm <sup>3</sup>	2.78 g/cm <sup>3</sup>	2.89 g/cm <sup>3</sup>
T <sub>g</sub>	719°C	515°C	527°C

<sup>a</sup> Referred to as “Collins-CL waste” composition.

<sup>b</sup> Referred to as “Collins-CLT waste” composition.

<sup>c</sup> Referred to as “Bakel waste” composition.

<sup>d</sup> Elemental concentrations of cesium and strontium were 5.36% and 1.77%, respectively.

<sup>e</sup> Elemental concentrations of cesium and strontium were 1.65% and 0.56%, respectively.

<sup>f</sup> Elemental concentrations of cesium and strontium were 2.57% and 0.88%, respectively.

**TABLE 2 Lanthanide isotope mass and decay power (from ORIGEN for 20-y cooled PWR fuel).**

Isotope	Mass (g/MTHM)	Power (W/MTHM)		Isotope	Mass (g/MTHM)	Power (W/MTHM)	
		From $\beta$ -rays	From $\gamma$ -rays			From $\beta$ -rays	From $\gamma$ -rays
La-138	$1.31 \times 10^{-2}$	$1.61 \times 10^{-12}$	$1.61 \times 10^{-12}$	Eu-152	$2.11 \times 10^{-2}$	$2.26 \times 10^{-2}$	$1.29 \times 10^{-2}$
La-139	$1.87 \times 10^3$	0	0	Eu-153	$1.93 \times 10^2$	0	0
Ce-140	$1.94 \times 10^3$	0	0	Eu-154	$1.93 \times 10^1$	$4.63 \times 10^1$	$3.86 \times 10^1$
Ce-142	$1.75 \times 10^3$	0	0	Eu-155	$6.11 \times 10^{-1}$	$2.48 \times 10^{-1}$	$1.52 \times 10^{-1}$
Ce-144	$8.13 \times 10^{-6}$	$1.72 \times 10^{-5}$	$4.44 \times 10^{-6}$	Gd-152	$2.20 \times 10^{-1}$	0	0
Pr-141	$1.73 \times 10^3$	0	0	Gd-153	$1.44 \times 10^{-11}$	$3.63 \times 10^{-11}$	$3.63 \times 10^{-11}$
Nd-142	$4.84 \times 10^1$	0	0	Gd-154	$8.47 \times 10^1$	0	0
Nd-143	$1.08 \times 10^3$	0	0	Gd-155	$1.05 \times 10^1$	0	0
Nd-144	$2.17 \times 10^3$	0	0	Gd-156	$2.14 \times 10^2$	0	0
Nd-145	$9.76 \times 10^2$	0	0	Gd-157	$5.83 \times 10^{-2}$	0	0
Nd-146	$1.12 \times 10^3$	0	0	Gd-158	$2.34 \times 10^1$	0	0
Nd-148	$5.60 \times 10^2$	0	0	Gd-160	2.00	0	0
Nd-150	$2.71 \times 10^2$	0	0	Tb-159	2.47	0	0
Pm-147	$5.28 \times 10^{-1}$	$1.83 \times 10^{-1}$	$3.66 \times 10^{-4}$	Dy-160	$8.98 \times 10^{-1}$	0	0
Sm-147	$1.53 \times 10^2$	0	0	Dy-161	$4.16 \times 10^{-1}$	0	0
Sm-148	$2.81 \times 10^2$	0	0	Dy-162	$3.09 \times 10^{-1}$	0	0
Sm-149	8.77	0	0	Dy-163	$4.01 \times 10^{-1}$	0	0
Sm-150	$5.88 \times 10^2$	0	0	Dy-164	$1.70 \times 10^{-1}$	0	0
Sm-151	$5.01 \times 10^1$	$1.51 \times 10^{-1}$	$3.03 \times 10^{-3}$	Ho-165	$3.14 \times 10^{-1}$	0	0
Sm-152	$1.12 \times 10^2$	0	0	Ho-166m	$2.10 \times 10^{-3}$	$2.75 \times 10^{-5}$	$1.76 \times 10^{-5}$
Sm-154	$5.43 \times 10^1$	0	0	Er-166	$1.06 \times 10^{-1}$	0	0
Eu-151	8.11	0	0	Er-167	$2.75 \times 10^{-2}$	0	0

**TABLE 3 Mass and power from lanthanide fission products (from ORIGEN, 20-y cooled PWR fuel). Power is dominated by europium but is still small compared to cesium and strontium decay.**

Lanthanide	Mass (g/MTHM)	Power (W/MTHM)	
		From $\beta$ -rays	From $\gamma$ -rays
La	$1.87 \times 10^3$	$1.61 \times 10^{-12}$	$1.61 \times 10^{-12}$
Ce	$3.69 \times 10^3$	$1.72 \times 10^{-5}$	$4.44 \times 10^{-6}$
Pr	$1.73 \times 10^3$	$1.99 \times 10^{-4}$	$4.90 \times 10^{-6}$
Nd	$6.22 \times 10^3$	0	0
Pm	$5.28 \times 10^{-1}$	$1.83 \times 10^{-1}$	$3.66 \times 10^{-4}$
Sm	$1.25 \times 10^3$	$1.51 \times 10^{-1}$	$3.03 \times 10^{-3}$
Eu	$2.21 \times 10^2$	$4.65 \times 10^1$	$3.88 \times 10^1$
Gd	$3.35 \times 10^2$	$3.63 \times 10^{-11}$	$3.63 \times 10^{-11}$
Tb	2.47	0	0
Dy	2.19	0	0
Ho	$3.16 \times 10^{-1}$	$2.75 \times 10^{-5}$	$1.76 \times 10^{-5}$
Er	$1.33 \times 10^{-1}$	0	0
Totals	15,324	47	39
Total specific power		0.0056 W/g of lanthanides	

**TABLE 4 Mass and power from transition metal fission products (from ORIGEN, 20-y cooled PWR fuel).**

Transition Metal	Mass (g/MTHM)	Power (W/MTHM)	
		From $\beta$ -rays	From $\gamma$ -rays
Cd	$1.59 \times 10^2$	$4.03 \times 10^{-2}$	$1.78 \times 10^{-2}$
Fe	$9.76 \times 10^3$	$4.19 \times 10^{-2}$	0
Ga	$2.43 \times 10^{-2}$	0	0
Mo	$5.21 \times 10^3$	0	0
Pd	$2.36 \times 10^3$	$9.80 \times 10^{-6}$	$9.80 \times 10^{-8}$
Rh	$5.04 \times 10^2$	$7.75 \times 10^{-3}$	$9.37 \times 10^{-4}$
Ru	$3.36 \times 10^3$	$4.71 \times 10^{-5}$	0
Sb	$1.25 \times 10^1$	$3.15 \times 10^{-1}$	$2.61 \times 10^{-1}$
Sn	$7.50 \times 10^1$	$9.84 \times 10^{-4}$	$4.35 \times 10^{-4}$
Te	$7.18 \times 10^2$	$1.97 \times 10^{-2}$	$1.97 \times 10^{-2}$
Zn	$4.09 \times 10^1$	0	0
Zr	$5.76 \times 10^3$	$3.29 \times 10^{-4}$	$1.22 \times 10^{-4}$

Cesium and strontium isotopes did significantly affect the thermal source term for the heat transfer calculations. For the calculation of mass and power per MTHM for the cesium and strontium isotopes (Table 5), 100% absorption of  $\gamma$ - and  $\beta$ -emissions [Kaminski-2005] was assumed. Depending on the size of the waste form, some  $\gamma$ -rays may escape the waste form, thereby not contributing toward the heat source term. For the range of fractional  $\gamma$ -ray absorption  $f_\gamma = 0.5$ -1.0, we determined the heat source terms for cesium (Fig. 1). The only strontium isotope of importance in the fuel is Sr-90, and because it is a pure  $\beta$ -emitter, the heat source term from strontium is not affected by  $\gamma$ -ray absorption.

**TABLE 5 Mass and power values used in the thermal calculations.**

Element	10-y Cooled Fuel		20-y Cooled Fuel		50-y Cooled Fuel	
	g/MTHM	W/MTHM	g/MTHM	W/MTHM	g/MTHM	W/MTHM
Cs <sup>a,b</sup>	3340	823	3018	501	2358	247
Sr <sup>c</sup>	1182	501	1044	394	750	191

<sup>a</sup> Cs-137 includes contributions from the short-lived daughter Ba-137m. The  $\gamma$ -ray emission was 661.66 keV (94.4% yield), and the  $\beta$ -ray emissions were 514 keV (94.4% yield) and 1175 keV (5.6% yield).

<sup>b</sup> Cs-134 included the following  $\gamma$ -ray emissions: 604.7 keV (97.56% yield), 795.9 keV (85.44% yield), 569.3 keV (15.43% yield), (8.38% yield); and the following  $\beta$ -ray emissions: 658 keV (70% yield) and 88.6 keV (27% yield).

<sup>c</sup> Sr-90 included contributions from the short-lived daughter Y-90. The  $\beta$ -ray emissions were 546 keV (100% yield) and 2282 keV (100% yield), where 1/3 the peak energy was taken as the average energy for the forthcoming calculations.

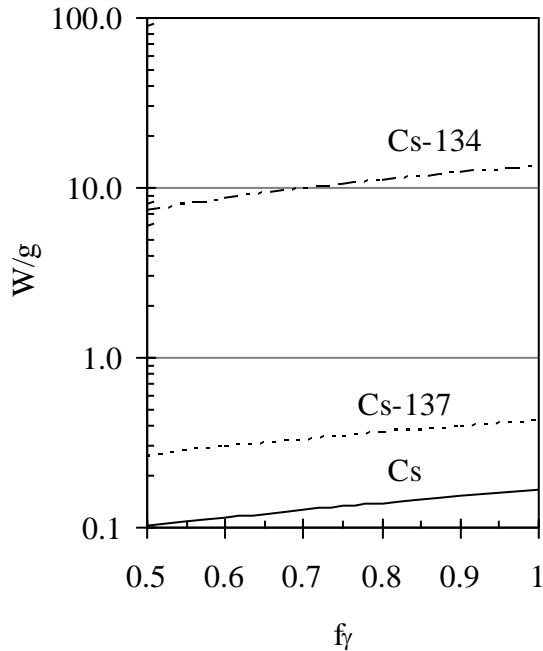


**FIGURE 1 Specific power of Cs-134, Cs-137, and total cesium a function of fraction of  $\gamma$ -rays deposited within a canister (isotopes from 20-y cooled fuel).**

The model requires several simplifying assumptions to arrive at an analytical solution:

- The waste is separated from dissolved PWR fuel burned to 50 GWd/MT (4.25%  $^{235}\text{U}$  enrichment).
- The waste form is fabricated immediately after the designated cooling period for the fuel (10, 20, or 50 y).
- The temperatures quoted are for waste forms at steady state with the coolant.
- The waste form is a smooth right cylinder.
- The baseline diameter of the waste form is 0.6 m (24 in.).
- The waste form length is fixed at 0.4 m (15 in.).
- The waste form is packaged in single-wall metal container with wall thickness of 2 cm (0.8 in.) and thermal conductivity ( $k$ ) of 22 W/(m·K) (typical of Zircaloy).

- The waste form porosity has a baseline value of zero. To handle cracks within the solidified glass, a homogeneous distribution of pores was assumed such that  $k$  can be estimated from an expression derived by Krupitzka [1967].
- The thermal conductivity ( $k = 1 \text{ W} \cdot \text{m}^{-1} \text{K}^{-1}$ ) and density of the waste forms do not change with waste loading.
- Contact between the waste form and its canister is intimate, with a convective heat transfer coefficient of  $1000 \text{ W}/(\text{m}^2 \cdot \text{K})$ .
- To cool the waste package, the air and water inlet temperatures are  $90^\circ\text{C}$  and  $40^\circ\text{C}$ , respectively.
- The waste forms are placed horizontally as single packages in the coolant flow. This assumption was not used in Section 3.3, where the effect of coolant heating is discussed.
- For active air cooling of the waste package, the convective heat transfer coefficient was fixed at  $50 \text{ W}/(\text{m}^2 \cdot \text{K})$ .
- The emissivity  $\varepsilon$  of the canister is 0.3.

### 3 RESULTS AND DISCUSSION

We estimated the radial temperature profile within right cylindrical glass monoliths for various waste loadings, radioactive decay powers, waste form diameters, and storage/disposal conditions. We evaluated three waste glasses. The first, CSLN-7C, contained only the cesium/strontium stream and the lanthanide elements. The second and third glasses contained these plus the transition metals in different concentrations. The waste loading in CSLNTM-C-2.5 was limited by high  $\text{MoO}_3$  while the waste loading in CSLNTM-B-3.0 was limited by high noble metals. The calculated data are presented in Figs. 2-7 and in the Appendix.

#### 3.1 EQUILIBRIUM CENTERLINE TEMPERATURES FOR BENCHMARK GLASSES

In the first evaluation, we calculated the maximum diameter at which  $T_{\text{centerline}}$  did not exceed the  $T_g$  measured by Crum et al. [2009] for that waste glass composition (Fig. 2). The waste form CSLN-7C ( $T_g = 719^\circ\text{C}$ ) is the most heat limiting of the three evaluated due to the high concentration of cesium (5.36%) and strontium (1.77%). Its diameter, when loaded with waste from 10-y cooled fuel, cannot exceed 0.278 m (10.94 in.). In comparison, the CSLNTM-C-2.5 can be made to 0.470 m (18.5 in.), and CSLNTM-B-3.0 can be made to 0.181 m (14.2 in.). The number of canisters that would need to be filled per 1000 MTHM processed from 10-y cooled fuel is 67, 92, and 96 for CSLN-7C, CSLNTM-C-2.5, and CSLNTM-B-3.0, respectively.

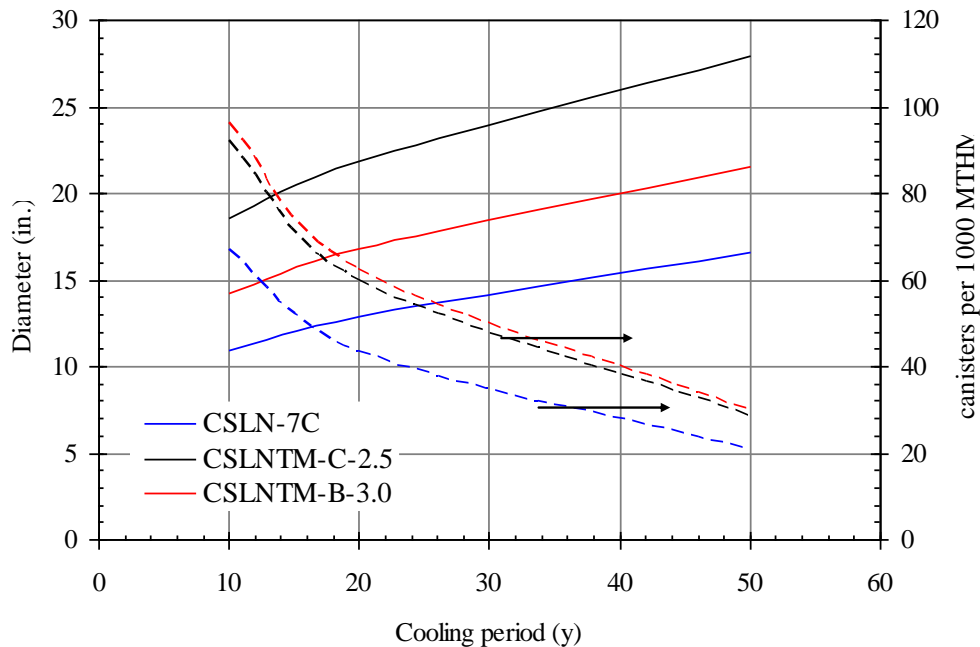


**FIGURE 2 Waste form diameter and required number of 4.6-m (15-ft) long canisters per 1000 MTHM processed per year for three candidate waste glass compositions as a function of the cooling period prior to processing fuel. The diameter was calculated based on  $T_{\text{centerline}} = T_g$ . Lines are color coded to the baseline waste glass composition.**



The waste form diameters can be dramatically increased when cooler fuel is used. For 50-y cooled fuel, the maximum diameter was 0.422 m (16.6 in.), 0.709 m (27.9 in.), and 0.546 m (21.5 in.) for CSLN-7C, CSLNTM-C-2.5, and CSLNTM-B-3.0, respectively. The number of canisters that need to be filled per 1000 MTHM was 21, 29, and 30 for these same glasses.

To observe the effect of waste form diameter on resulting centerline temperatures, we computed the equilibrium temperatures for the three waste glasses with diameter of ~0.30 m (12.0 in.) to 0.61 m (24.0 in.) (Fig. 3). The  $T_g$  is shown for each waste glass composition as a function of diameter. Including a safety factor to ensure the waste form temperature remains below  $T_g$  under loss-of-coolant conditions or changes in the physical properties of the waste form during storage would result in a significant decrease in the diameter. For example, let us assume that a safety factor of 20% with respect to centerline temperature is required. For the CSLNTM-B-3.0 composition ( $T_g = 527^\circ\text{C}$  and 20% safety factor =  $421^\circ\text{C}$ ), the waste form diameter from 10-yr cooled fuel would be 0.305 m (12.0 in.) compared to 0.36 m (14.2 in.) at  $T_g$ ; from 20-y cooled fuel, the diameter would be 0.366 m (14.4 in.) compared to 0.427 m (16.8 in.) at  $T_g$ ; and from 50-y cooled fuel, the diameter would be 0.465 m (18.3 in.) compared to 0.546 (21.5 in.) at  $T_g$ .

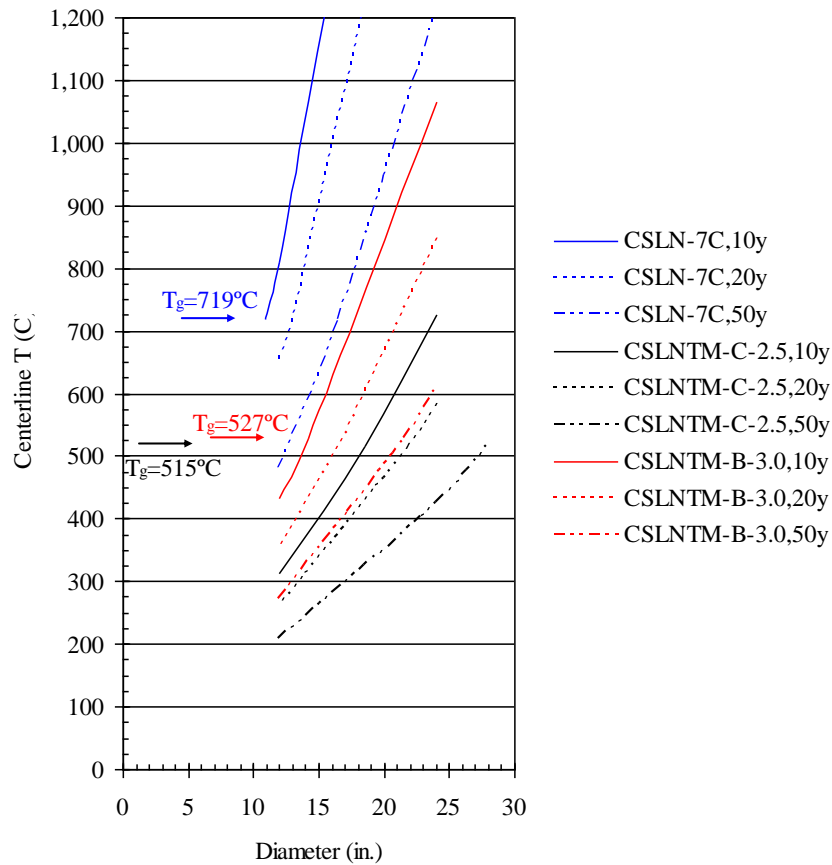


**FIGURE 3 Centerline temperature ( $^\circ\text{C}$ ) for different diameter glasses for the three baseline waste glass compositions.**

Because the specific power (W/g) of the waste form ( $P$ ) is one of the primary drivers in computing the centerline temperature, we plotted  $T_{\text{centerline}}$  of the three waste glass compositions as a function of the power generated in each canister (Fig. 4). The resulting plot shows good correlations, which can be represented by simple linear functions regardless of the age of the original fuel.

For CSLN-7C,

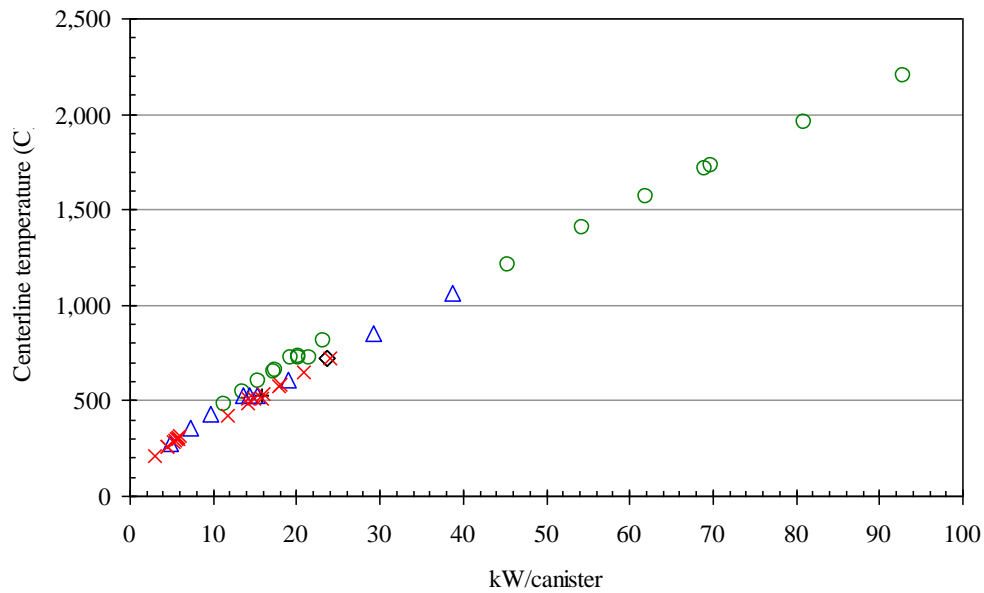
$$T_{\text{centerline}} (^{\circ}\text{C}) = 20.6 P \left[ \frac{\text{kW}}{\text{canister}} \right] + 292 \quad (R^2=0.9988). \quad (2)$$

For CSLNTM-C-2.5,

$$T_{\text{centerline}} (^{\circ}\text{C}) = 23.4 P \left[ \frac{\text{kW}}{\text{canister}} \right] + 162 \quad (R^2=0.9955). \quad (3)$$

For CSLNTM-B-3.0,

$$T_{\text{centerline}} (^{\circ}\text{C}) = 22.6 P \left[ \frac{\text{kW}}{\text{canister}} \right] + 193 \quad (R^2=0.995). \quad (4)$$



If we focus on centerline temperatures  $< 800^{\circ}\text{C}$  and force the line to pass through the origin, the resulting second-order polynomial line fit is

$$T_{\text{centerline}} (^{\circ}\text{C}) = -0.876 \left( P \left[ \frac{\text{kW}}{\text{canister}} \right] \right)^2 + 51.2 P \left[ \frac{\text{kW}}{\text{canister}} \right] \quad (R^2=0.925). \quad (5)$$

The fit of the data only (ignoring the origin, Fig. 5) is

$$T_{\text{centerline}} (^{\circ}\text{C}) = -0.114 \left( P \left[ \frac{\text{kW}}{\text{canister}} \right] \right)^2 + 28.9 P \left[ \frac{\text{kW}}{\text{canister}} \right] + 139 \quad (R^2=0.960). \quad (6)$$

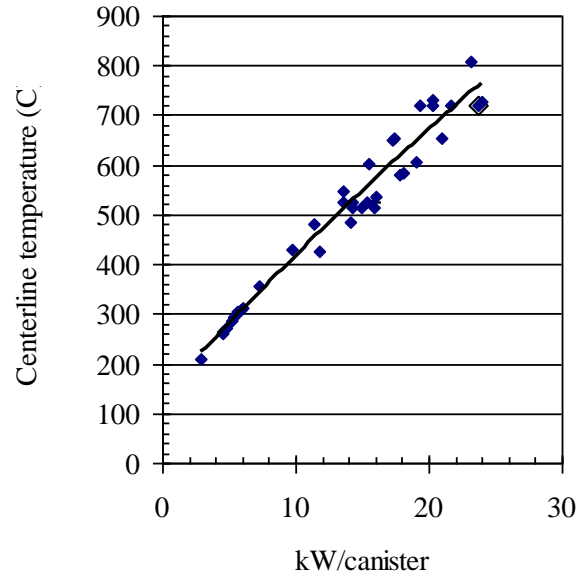


**FIGURE 5** Aggregate of equilibrium centerline temperature data for the three waste form glasses for  $T_{\text{centerline}} \leq 800^{\circ}\text{C}$ . Line fit of data is for second-order polynomial.

### 3.2 $\gamma$ -RAY ABSORPTION

In the previous calculations, we employed a conservative value for the heat source since we assumed 100% absorption of  $\gamma$ -rays within the waste form. However, absorption will be somewhat smaller than this value. Consider that the half-thickness<sup>1</sup> of borosilicate glass for 662 keV  $\gamma$ -rays (primary  $\gamma$ -ray in the Cs-137 decay chain) is approximately 0.08 m (3 in.). We calculated the relative equilibrium centerline temperature for a 0.305-m (12-in.) diameter canister with the CSLNTM-C-2.5 composition, where the fraction of  $\gamma$ -rays absorbed within the canister was varied between 0.5 and 1.0. This resulted in an equilibrium centerline temperature range of 262 to 313°C (Fig. 6).

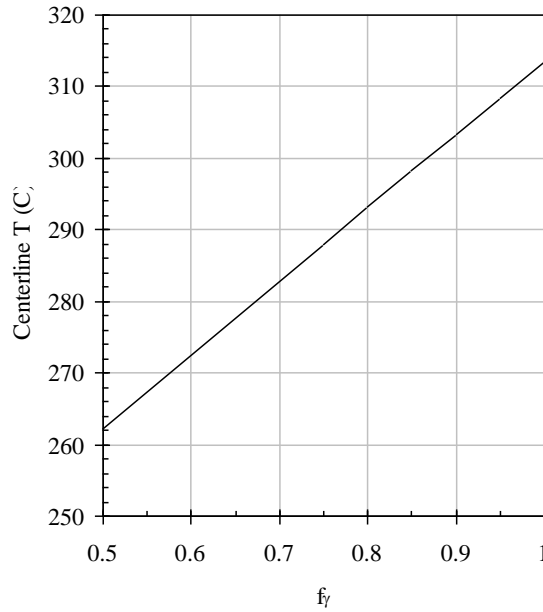


**FIGURE 6** Equilibrium centerline temperature of CSLNTM-C-2.5, assuming increasing value for fraction of  $\gamma$ -rays absorbed within the waste form.

Another important factor is the effect of the thermal conductivity on the equilibrium temperature. The thermal conductivity of glasses varies with composition, and the thermal conductivities for lanthanide borosilicate glasses are not known. In our baseline case, we assumed  $k = 1.0 \text{ W/(m}\cdot\text{K)}$  for all glasses based on estimates provided by PNNL [J. Vienna, personal communication]. Starting with the glasses at  $T_{\text{centerline}} = T_g$  prepared from 20-y cooled fuel (see Fig. 3), we determined  $T_{\text{centerline}}$  as a function of  $k$  for the three baseline glass compositions, which have yet to be measured experimentally. Note that the relationship is not

<sup>1</sup> Based on mass energy absorption coefficient ( $\mu/\rho$ ) for Pyrex borosilicate glass of  $0.08755 \text{ cm}^2/\text{g}$  at 662 keV, density of  $3 \text{ g/cm}^3$ , and the relation  $E(x) = E_0 e^{-(\mu/\rho)\rho x}$ , where  $x$  is the thickness of the absorber glass [NIST-2009].

linear, with  $-dT/dk$  being much larger for  $k < 1$  W/(m·K) than for  $k > 1$  W/(m·K). For  $k = 0.8$  W/(m·K), the  $T_{\text{centerline}}$  increases by 90°C for the CSLN-7C waste form (719 to 807°C) and 60°C for the two CSLNTM waste forms. In contrast, for  $k = 1.2$  W/(m·K),  $T_{\text{centerline}}$  is reduced by 50°C for CSLN-7C (719 to 660°C) and 40°C for CSLNTM. Doubling the baseline value of  $k$  will result in a decrease of 175°C for CSLN-7C and ~125°C for CSLNTM.

### 3.3 EFFECT OF CRACKING

Solidified glasses will inevitably produce significant cracking, which can increase the surface area of the glass by 25 times or more [Jones-2006]. The cracks may be present anywhere in the glass and can have varied distribution. In addition, void spaces may occur at the glass-canister interface. Because of the irregular occurrence and geometry of cracks, analytical models are difficult to construct. A cracking model described by Jernkvist [1997] relates an effective thermal conductivity in the radial direction  ${}_i k$  to the crack strain  ${}_i \varepsilon_c$ :

$${}_i k = k_0 \left( 1 + \frac{k_0}{k_g} {}_i \varepsilon_c \right)^{-1}, \quad (7)$$

where  $k_0$  is the  $k$  for the uncracked solid, and  $k_g$  is the  $k$  for the gas phase within the crack. Essentially, this equation relates the effective thermal conductivity to the occurrence of cracks given by  ${}_i \varepsilon_c$ . Since we have no data on  ${}_i \varepsilon_c$  for waste glass, we have used another method for estimating the effective thermal conductivity by modeling the cracks as a homogeneous distribution of pores. Introducing porosity produces the same effect of adjusting the thermal conductivity for the resistivity of the gas phase, although we have no expression to relate homogeneous porosity to heterogeneous cracking. Moreover, thermal transport through a medium containing homogeneous pores will be much different from transport through a cracked medium. In a homogeneously porous medium, the solid phase is continuous so that the majority of thermal energy is transported within the solid phase and around the pores. In a cracked medium, the continuity of the crack forces heat transport across a gap that will produce a temperature drop. Empirical formulas have been developed to account for cracking in nuclear fuel [Todreas-1990]. Although different phenomena will affect the heat transport of in-reactor  $\text{UO}_2$  compared with nuclear waste, we may use the resulting equations to provide a “feel” for potential values of  $k$ . The equations estimate a reduction in  $k$  by up to 20% at 500°C in  $\text{UO}_2$  fuel.

We modeled cracking by assuming a porosity fraction of 0.08-0.3. The resulting thermal conductivity and centerline temperature were calculated and are reported in Fig. 8. Essentially, this figure is an extension of Fig. 7 except that the reduction in density associated with adding porosity is taken into account. As discussed with regard to Fig. 7,  $T_{\text{centerline}}$  is particularly sensitive to thermal conductivity for  $k < 1$  W/(m·K). Given this sensitivity to  $k$ , experimental data specific to glass waste forms are needed to establish credible values of the effective thermal conductivity, and the potential importance of cracking to the stability of stored or disposed glasses.

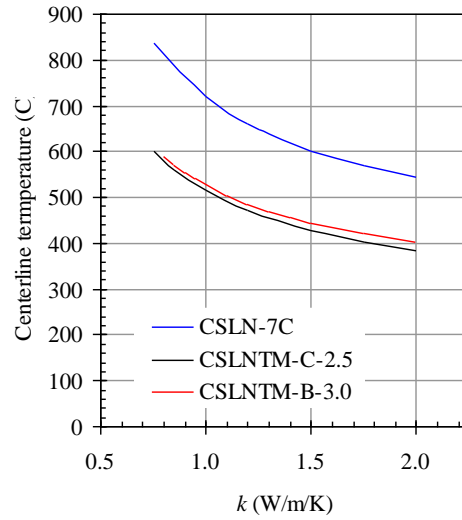


**FIGURE 7** Equilibrium centerline temperatures as function of thermal conductivity  $k$ .

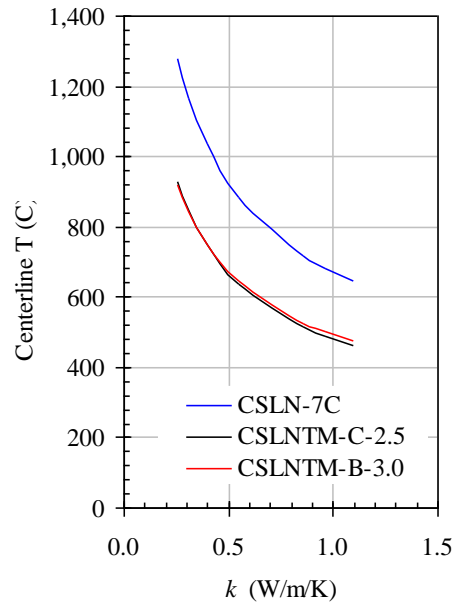


**FIGURE 8** Centerline temperature as a function of thermal conductivity for the three baseline waste glasses (from 20-y cooled fuel) with cracks. Cracks were modeled as fractional porosity from 0.08 to 0.3.

### 3.4 COOLANT HEATING ALONG VERTICAL ELEMENTS

In our calculations of the effects of coolant heating on waste forms, we assumed constant coolant temperature, which is more accurate for short waste cylinders or cylinders stored horizontally. We briefly investigated the effect of coolant temperature on the equilibrium glass centerline temperature. To that end, we used an estimate for the temperature of the coolant fluid as a function of  $z$  distance up the waste form,  $T_{fluid}(z)$  [AFCI-2006]:

$$T_{fluid}(z) = \frac{Pz}{\rho C_p v (R_{pitch}^2 - \pi R_{waste}^2)}, \quad (8)$$

where  $P$  is the linear power in W/m,  $\rho$  is the density of the fluid,  $C_p$  is the heat capacity of the fluid,  $R_{pitch}$  is the coolant channel pitch (assumed to be equal to  $2.5 \times R_{waste}$ ), and  $R_{waste}$  is the radius of the waste canister. In addition,  $v$  is the flow velocity, estimated by

$$v = \left( \frac{Nu}{0.023} \frac{1}{Pr^{0.4}} \right)^{1/0.8} \frac{\nu_{fluid}}{D}, \quad (9)$$

where  $Nu$  is the Nusselt number,  $Pr$  the Prandtl number,  $\nu$  is the kinematic viscosity of the fluid, and  $D$  is the diameter of the waste canister. Using these equations, we calculated the temperature along the axial direction for vertically emplaced waste cylinders, where the coolant flows from the bottom to the top of the 4.57-m (15-ft) long waste form. We used the extreme case of a 0.610-m (24-in.) diameter canister of CSLN-7C (from 20-y cooled fuel). The estimated results were 1728°C for the centerline at the bottom and 1754°C for the centerline at the top of the canister. Similarly, for the waste glass composition with low power density, CSLNTM-B-3.0 (from 20-y cooled fuel), the centerline temperature at the coolant inlet was 849°C and 876°C at the outlet. The same waste form at 0.305-m (12-in.) diameter produced centerline temperatures of 356°C at the inlet and 384°C at the outlet. Therefore, we estimate an axial  $\Delta T$  for the centerline temperature of 25-30°C for these waste glasses.

### 3.5 ACTIVE COOLING OF WASTE FORMS IN AIR AND PASSIVE COOLING IN WATER

In the analysis of active and passive waste cooling, we assumed the waste form diameters matched those that produced centerline temperatures equal to  $T_g$ . Then, the equilibrium temperature was re-calculated for forced convective cooling by air and passive cooling in water. As shown by the data in Table 6, compared with passive air cooling, cooling the waste forms in forced air decreases the centerline temperature of the waste forms by ~25%, and cooling in water reduces the centerline temperature by ~40%.

**TABLE 6 Equilibrium centerline temperatures for waste form glasses prepared from 20-y cooled fuel and cooled by air and water.**

Waste Glass Composition	Diameter at $T_g$	Equilibrium Temperature $T_{\text{centerline}}$		
		Baseline Case: Passive cooling in air	Active Cooling in Air	Passive Cooling in Water
CSLN-7C	0.328 m (12.9 in.)	719°C	520°C	408°C
CSNLTM-C-2.5	0.554 m (21.8 in.)	515°C	385°C	308°C
CSLNTM-B-3.0	0.426 m (16.8 in.)	527°C	383°C	299°C

### 3.6 EQUILIBRIUM TEMPERATURE FOR BURIED WASTE FORMS

To estimate the canister temperature when buried for disposal, we increased the canister wall thickness to 10 m (32 ft) with  $k = 0.25 \text{ W}/(\text{m}\cdot\text{K})$ , which is typical of compacted, dehydrated clay. For this analysis, we pursued several approaches. First, we calculated the diameter of the waste form such that the centerline temperature would not exceed  $T_g$  when buried (Table 7). The data indicate that burial of waste forms will result in an immediate temperature excursion due to the insulating character of earth, and the resulting diameters are not more than ~10 cm (4 in.).

**TABLE 7 Equilibrium centerline temperatures for waste form glasses prepared from 20-y cooled fuel and buried in earth.**

Waste Glass Composition	Diameter at $T_g$ Under Passive Air Cooling	Maximum Diameter in Earth ( $T_{\text{centerline}}=T_g$ )
CSLN-7C	0.328 m (12.9 in.)	0.064 m (2.52 in.)
CSNLTM-C-2.5	0.554 m (21.8 in.)	0.108 m (4.26 in.)
CSLNTM-B-3.0	0.426 m (16.8 in.)	0.0844 m (3.32 in.)



Next, we assumed that the waste form diameter was maintained at 0.610 m (24 in.). For the centerline temperature to not exceed  $T_g$ , we forced the waste feed to be diluted by some factor (relative to the baseline loading presented in Table 1) in order to reduce the specific power of the waste form. We calculated the dilution factors to be 14 to 75 depending on the composition and age of the fuel (Table 8).

**TABLE 8 Dilution factors of the waste feed required to produce a 0.610-m (24-in.) diameter waste form with  $T_{\text{centerline}} = T_g$  for glasses prepared from 10-, 20-, and 50-y cooled fuel and buried in earth.**

Waste Glass Composition	10-y Cooled Fuel	20-y Cooled Fuel	50-y Cooled Fuel
CSLN-7C	75	56	37
CSNLTM-C-2.5	29	22	14
CSLNTM-B-3.0	45	34	22

## 4 CONCLUSIONS

For this effort we estimated the equilibrium centerline temperatures for lanthanide borosilicate glass waste forms and examined the sensitivity of the centerline temperatures to changes in the waste form physical properties and mode of cooling. The dominant heat source in a waste containing a cesium/strontium stream, the lanthanides, and the transition metals is from the decay of Cs-134, Cs-137, Sr-90, and their daughters Ba-137m and Y-90.

The maximum diameters for the three baseline glasses from Table 1 [ $k = 1.0 \text{ W}/(\text{m}\cdot\text{K})$ ] prepared from 20-y cooled fuel were determined to be:

- 0.278 m (10.94 in.) for CSLN-7C
- 0.470 m (18.5 in.) for CSLNTM-C-2.5
- 0.181 m (14.2 in.) for CSLNTM-B-3.0

for  $T_{\text{centerline}}=T_g$  under passive cooling in air. At these values, the number of canisters required to dispose the waste from 1000 MTHM processed was 67, 92, and 96 for CSLN-7C, CSLNTM-C-2.5, and CSLNTM-B-3.0, respectively. The cooler waste from older fuel can be accommodated in larger diameter canisters [0.422 m (16.6 in.), 0.709 m (27.9 in.), and 0.546 m (21.5 in.) for CSLN-7C, CSLNTM-C-2.5, and CSLNTM-B-3.0, respectively], which reduces the number of canisters needed per 1000 MTHM by a factor of three.

We have modeled the centerline temperature of the baseline glasses as a function of total power within a canister ( $P$ ) by using a simple polynomial fit to the data in Fig. 5:

$$T_{\text{centerline}} \text{ (}^\circ\text{C)} = -0.114 \left( P \left[ \frac{kW}{\text{canister}} \right] \right)^2 + 28.9 P \left[ \frac{kW}{\text{canister}} \right] + 139 \quad (R^2 = 0.960)$$

for centerline temperatures  $< \sim 800^\circ\text{C}$ . This relationship applies to glass waste forms prepared from 10-, 20-, and 50-y cooled fuel.

We determined the sensitivity of the temperature function to changes in thermal conductivity either due to uncertainty in our measurement of the solidified glass or the effects of cracking. For the glasses at  $T_{\text{centerline}}=T_g$  prepared from 20-y cooled fuel (see Fig. 3), the relationship is not linear, with  $-dT/dk$  being much larger for  $k < 1 \text{ W}/(\text{m}\cdot\text{K})$  than for  $k > 1 \text{ W}/(\text{m}\cdot\text{K})$ . For  $k = 0.8 \text{ W}/(\text{m}\cdot\text{K})$ ,  $T_{\text{centerline}}$  increases by  $90^\circ\text{C}$  for CSLN-7C waste form (719 to  $807^\circ\text{C}$ ) and  $60^\circ\text{C}$  for the two CSLNTM waste forms. In contrast, for  $k = 1.2 \text{ W}/(\text{m}\cdot\text{K})$ ,  $T_{\text{centerline}}$  is reduced by  $50^\circ\text{C}$  for CSLN-7C (719 to  $660^\circ\text{C}$ ) and  $40^\circ\text{C}$  for the CSLNTM samples. Experimental data are required for us to properly evaluate the magnitude of cracking and quantify the values of the effective thermal conductivity of the cracked solid.

Finally, we showed that heating of the coolant fluid along a vertically emplaced waste form will result in a  $\Delta T_{\text{centerline}}$  along the z-axis of 25-30°C. However, active cooling by air will reduce the centerline temperatures by ~25%, and passive cooling in water will reduce  $T_{\text{centerline}}$  by ~40% over the baseline case of passive cooling in air. Also, we found that burial of fresh waste form glasses will require low waste loadings to avoid thermal heating to above the glass transition temperature, or the glasses must be cooled for prolonged periods prior to burial.

## **ACKNOWLEDGMENTS**

This work was conducted in support of Work Package AN0915030310 and describes activities associated with milestone M3503031001. Argonne National Laboratory is operated for the U.S. Department of Energy by UChicago Argonne, LLC, under contract DE-AC0Z-06CH11357.

## REFERENCES

- Advanced Fuel Cycle Initiative (AFCI). 2006. *AFCI Separations Technical Quarterly Report*, “Engineered Product Storage Technical Reports.”
- Crum, J. V., A. L. Billing, J. Lang, J. C. Marra, C. Rodriguez, J. V. Ryan, and J. D. Vienna. 2009. *Baseline Glass Development for Combined Fission Products Waste Streams*, AFCI-WAST-WAST-MI-DV-2009-000075.
- Gombert, D., et al. 2007. *Global Nuclear Energy Partnership Integrated Waste Treatment Strategy Waste Treatment Baseline Strategy*, GNEP-WAST-AI-RT-2007-000324.
- Jernkvist, L. O. 1997. “A continuum model for the mechanical behavior of UO<sub>2</sub> fuel under cracking, relocation and PCMI,” Transactions of the 14th International Conference on Structural Mechanics in Reactor Technology, Lyon, France, August 17-22, 1997.
- Jones, T., J. Marra, D. Immel, and B. Meers. 2006. *Glass Macrocracking Determination in Prototypic Canisters Containing Lanthanide Borosilicate Glass*, Savannah River National Laboratory Report WSRC-TR-2006-00015, Revision 0.
- Kaminski, M. D. 2005. “Engineering product storage under the Advanced Fuel Cycle Initiative. Part I: An iterative thermal transport modeling scheme for high-heat-generating radioactive storage forms,” J. Nucl. Mater. 347: 94–103.
- Krupiczka, R. 1967. “Analysis of effective thermal conductivity of granular materials,” Int. Chem. Eng. 7: 122–144.
- National Institute of Standards and Technology (NIST). 2009. *X-Ray Mass Attenuation Coefficients*, <http://physics.nist.gov/PhysRefData/XrayMassCoef/tab4.html>.
- Todreas, N. E., and M. S. Kazimi. 1990. *Nuclear Systems, I: Thermal Hydraulic Fundamentals*, Taylor and Francis Publishing, London, pp. 303–310.

**APPENDIX A**  
**SUMMARY DATA FOR WASTE FORMS**

**TABLE A-1 Data for CSLN-7C at constant  $k = 1.0 \text{ W/(m}\cdot\text{K)}$  (waste form density=3.36 g/cm<sup>3</sup>,  $T_g = 719^\circ\text{C}$ ).**

Radius (m)	ID (in.)	$f_g$	Dilution Factor	Centerline Temp. (°C)	Surface Temp. (°C)	kg per can	kW/ can	$h_{conv}$	$h_{rad}$	$h_{tot}$	Fuel Cooled (y)	Cans/ 1000 MTHM	$h_{conv}$ notes <sup>a</sup>
0.3048	24.0	0.5	1.00	1,711	495	4,484	69.0	4.38	13.88	18.27	10	14	p. air
0.3048	24.0	0.75	1.00	1,956	530	4,484	81.0	4.33	15.39	19.73	10	14	p. air
0.3048	24.0	1	1.00	2,197	561	4,484	92.9	4.28	16.85	21.13	10	14	p. air
0.3048	24.0	0.5	1.00	1,404	446	4,484	54.4	4.45	11.93	16.38	20	13	p. air
0.3048	24.0	0.75	1.00	1,567	473	4,484	62.1	4.42	12.97	17.39	20	13	p. air
0.3048	24.0	1	1.00	1,728	497	4,484	69.8	4.38	13.98	18.36	20	13	p. air
0.3048	24.0	1	1.00	1,212	411	4,484	45.5	4.49	10.68	15.17	50	10	p. air
0.1524	12.0	0.5	1.00	650	342	1,121	17.3	5.33	8.49	13.82	10	56	p. air
0.1524	12.0	0.75	1.00	730	369	1,121	20.2	5.31	9.31	14.62	10	56	p. air
0.1524	12.0	1	1.00	808	394	1,121	23.2	5.28	10.12	15.40	10	56	p. air
0.1524	12.0	0.5	1.00	547	305	1,121	13.6	5.34	7.45	12.79	20	50	p. air
0.1524	12.0	0.75	1.00	602	325	1,121	15.5	5.34	8.00	13.34	20	50	p. air
0.1524	12.0	1	1.00	655	344	1,121	17.5	5.33	8.54	13.87	20	50	p. air
0.1524	12.0	1	1.00	482	279	1,121	11.4	5.33	6.80	12.13	50	39	p. air
0.13895	10.94	1	1.00	719	374	932	19.3	5.41	9.46	14.88	10	67	p. air
0.16406	12.92	1	1.00	719	359	1,299	20.2	5.23	8.99	14.22	20	43	p. air
0.21017	16.55	1	1.00	719	336	2,132	21.6	4.96	8.32	13.28	50	21	p. air
0.13895	10.94	1	1.00	512	168	932	19.3	50.00	4.46	54.46	10	67	a. air
0.16406	12.92	1	1.00	520	160	1,299	20.2	50.00	4.33	54.33	20	43	a. air
0.13895	10.94	1	1.00	393	49	932	19.3	3.73	2.17	5.91	10	67	p. water
0.16406	12.92	1	1.00	408	48	1,299	20.2	3.56	2.17	5.73	20	43	p. water
0.3048	24.0	1	3.93	719	302	4,484	23.7	4.56	7.38	11.94	10	55	p. air
0.3048	24.0	1	2.95	719	302	4,484	23.7	4.56	7.38	11.94	20	37	p. air
0.02734	2.15	1	1.00	719	91	36	0.7	0.60	3.26	3.87	10	1729	Ground
0.03195	2.52	1	1.00	719	91	49	0.8	0.61	3.26	3.87	20	1144	Ground
0.04041	3.18	1	1.00	719	91	79	0.8	0.61	3.26	3.88	50	559	Ground
0.3048	24.0	1	75.09	719	91	4,484	1.2	0.67	3.27	3.94	10	1045	Ground
0.3048	24.0	1	56.45	719	91	4,484	1.2	0.67	3.27	3.94	20	709	Ground
0.3048	24.0	1	36.76	719	91	4,484	1.2	0.67	3.27	3.94	50	361	Ground

<sup>a</sup> Abbreviations: “p. air” = passively cooled in air; “a. air” = actively cooled in air; “p. water” = passively cooled in water; “ground” = buried waste form is cooled by conductive heat transfer through earth.

**TABLE A-2 Data for CSLN-7C as function of  $k$**   
**[waste form density = 3.36 g/cm<sup>3</sup>,  $T_g = 719^\circ\text{C}$ ,**  
**diameter = 0.328 m (12.9 in.)]**

$k$ or $k$ effective [W/(m·K)]	$p$	Centerline Temp. ( $^\circ\text{C}$ )	Surface Temp. ( $^\circ\text{C}$ )
1.10	0.08	648	345
0.96	0.09	683	343
0.86	0.1	719	341
0.55	0.15	886	332
0.40	0.2	1,037	322
0.31	0.25	1,168	312
0.25	0.3	1,278	302
0.75	0	837	359
0.80	0	807	359
1.00	0	719	359
1.20	0	661	359
1.25	0	649	359
1.50	0	602	359
1.75	0	568	359
2.00	0	543	359



**TABLE A-3 Data for CSLNTM-C-2.5 at constant  $k = 1.0 \text{ W/(m}\cdot\text{K)}$  (waste form density =  $2.78 \text{ g/cm}^3$ ,  $T_g = 515^\circ\text{C}$ ).**

Radius (m)	ID (in.)	$f_g$	Dilution Factor	Centerline Temp. ( $^\circ\text{C}$ )	Surface Temp. ( $^\circ\text{C}$ )	kg per can	kW/ can	$h_{conv}$	$h_{rad}$	$h_{tot}$	Fuel Cooled (y)	Cans/ 1000 MTHM	$h_{conv}$ notes <sup>a</sup>
0.3048	24.0	0.5	1.00	579	264	3,710	17.9	4.54	6.44	10.98	10	55	p. air
0.3048	24.0	0.75	1.00	653	285	3,710	20.9	4.55	6.94	11.49	10	55	p. air
0.3048	24.0	1	1.00	726	304	3,710	23.9	4.56	7.43	11.99	10	55	p. air
0.3048	24.0	0.5	1.00	485	237	3,710	14.1	4.49	5.81	10.31	20	49	p. air
0.3048	24.0	0.75	1.00	535	252	3,710	16.1	4.52	6.14	10.66	20	49	p. air
0.3048	24.0	1	1.00	583	266	3,710	18.0	4.54	6.47	11.01	20	49	p. air
0.3048	24.0	1	1.00	425	218	3,710	11.7	4.44	5.41	9.86	50	39	p. air
0.1524	12.0	0.5	1.00	262	183	927	4.5	5.03	4.72	9.75	10	219	p. air
0.1524	12.0	0.75	1.00	288	195	927	5.2	5.10	4.96	10.06	10	219	p. air
0.1524	12.0	0.8	1.00	293	197	927	5.4	5.12	5.00	10.12	10	219	p. air
0.1524	12.0	0.85	1.00	298	200	927	5.5	5.13	5.05	10.18	10	219	p. air
0.1524	12.0	0.9	1.00	303	202	927	5.7	5.14	5.10	10.24	10	219	p. air
0.1524	12.0	0.95	1.00	308	204	927	5.8	5.15	5.14	10.29	10	219	p. air
0.1524	12.0	1	1.00	313	207	927	6.0	5.16	5.19	10.35	10	219	p. air
0.1524	12.0	1	1.00	264	183	927	4.5	5.03	4.74	9.77	20	197	p. air
0.1524	12.0	1	1.00	208	156	927	2.9	4.78	4.25	9.03	50	154	p. air
0.23515	18.52	1	1.00	515	263	2,208	14.2	4.82	6.41	11.23	10	92	p. air
0.2771	21.82	1	1.00	515	252	3,066	14.9	4.62	6.15	10.78	20	60	p. air
0.3543	27.90	1	1.00	515	236	5,012	15.9	4.33	5.79	10.13	50	29	p. air
0.23515	18.52	1	1.00	378	126	2,208	14.2	50.00	3.77	53.77	10	92	a. air
0.27710	21.82	1	1.00	385	123	3,066	14.9	50.00	3.72	53.72	20	60	a. air
0.23515	18.52	1	1.00	297	45	2,208	14.2	50.00	2.14	52.14	10	92	p. water
0.27710	21.82	1	1.00	308	45	3,066	14.9	50.00	2.13	52.13	20	60	p. water
0.3048	24.0	1	1.57	515	246	3,710	15.3	4.51	6.01	10.52	10	86	p. air
0.3048	24.0	1	1.18	515	246	3,710	15.3	4.51	6.01	10.52	20	58	p. air
0.04635	3.65	1	1.00	515	91	86	0.6	0.56	3.26	3.82	10	2363	Ground
0.05416	4.26	1	1.00	515	91	117	0.6	0.57	3.26	3.83	20	1563	Ground
0.06864	5.40	1	1.00	515	91	188	0.6	0.57	3.26	3.83	50	761	Ground
0.3048	24.0	1	28.64	515	91	3,710	0.8	0.61	3.26	3.88	10	1565	Ground
0.3048	24.0	1	21.58	515	91	3,710	0.8	0.61	3.26	3.88	20	1065	Ground
0.3048	24.0	1	14.06	515	91	3,710	0.8	0.61	3.26	3.88	50	542	Ground

<sup>a</sup> Abbreviations: “p. air” = passively cooled in air; “a. air” = actively cooled in air; “p. water” = passively cooled in water; “ground” = buried waste form is cooled by conductive heat transfer through earth.

**TABLE A-4 Data for CSLNTM-C-2.5 as function of  $k$  [waste form density = 2.78 g/cm<sup>3</sup>,  $T_g = 515^\circ\text{C}$ , diameter = 0.554 m (21.8 in.)].**

$k$ or $k$ effective [W/(m·K)]	$p$	Centerline Temp. ( $^\circ\text{C}$ )	Surface Temp. ( $^\circ\text{C}$ )
1.10	0.08	463	242
0.96	0.09	489	241
0.86	0.1	515	240
0.55	0.15	639	234
0.40	0.2	750	227
0.31	0.25	848	221
0.25	0.3	929	214
0.75	0	602	252
0.85	0	561	252
1.00	0	515	252
1.20	0	472	252
1.50	0	429	252
1.75	0	404	252
2.00	0	385	252

**TABLE A-5 Data for CSLNTM-B-3.0 at constant  $k = 1.0 \text{ W/(m}\cdot\text{K)}$  (waste form density =  $2.89 \text{ g/cm}^3$ ,  $T_g = 527^\circ\text{C}$ ).**

Radius (m)	ID (in.)	$f_g$	Dilution Factor	Centerline Temp. ( $^\circ\text{C}$ )	Surface Temp. ( $^\circ\text{C}$ )	kg per can	kW/ can	$h_{conv}$	$h_{rad}$	$h_{tot}$	Fuel cooled (y)	Cans/ 1000 MTHM	$h_{conv}$ notes <sup>a</sup>
0.3048	24.0	1	1.00	1,065	382	3,856	38.8	4.52	9.71	14.23	10	34	p. air
0.3048	24.0	1	1.00	849	334	3,856	29.2	4.55	8.26	12.81	20	30	p. air
0.3048	24.0	1	1.00	608	272	3,856	19.0	4.54	6.63	11.18	50	24	p. air
0.1524	12.0	1	1.00	431	259	964	9.7	5.31	6.30	11.61	10	135	p. air
0.1524	12.0	1	1.00	356	226	964	7.3	5.23	5.59	10.82	20	122	p. air
0.1524	12.0	1	1.00	272	187	964	4.8	5.06	4.81	9.87	50	95	p. air
0.18054	14.22	1	1.00	527	285	1,353	13.6	5.14	6.95	12.09	10	96	p. air
0.2132	16.79	1	1.00	527	274	1,887	14.3	4.94	6.67	11.60	20	62	p. air
0.2735	21.54	1	1.00	527	257	3,106	15.3	4.64	6.26	10.90	50	30	p. air
0.1805	14.22	1	1.00	375	134	1,353	13.6	50.00	3.89	53.89	10	96	a. air
0.2132	16.79	1	1.00	383	130	1,887	14.3	50.00	3.83	53.83	20	62	a. air
0.18054	14.22	1	1.00	287	46	1,353	13.6	3.19	2.14	5.33	10	96	p. water
0.2132	16.79	1	1.00	299	45	1,887	14.3	3.03	2.14	5.17	20	62	p. water
0.3048	24.00	1	2.46	527	249	3,856	15.8	4.52	6.09	10.61	10	83	p. air
0.3048	24.00	1	1.85	527	249	3,856	15.8	4.52	6.09	10.61	20	56	p. air
0.03611	2.84	1	1.00	527	90	54	0.5	0.56	3.26	3.82	10	2400	Ground
0.04218	3.32	1	1.00	527	91	74	0.6	0.56	3.26	3.82	20	1589	Ground
0.3048	24.0	1	45.13	527	91	3,856	0.9	0.62	3.26	3.88	10	1521	Ground
0.3048	24.0	1	33.99	527	91	3,856	0.9	0.62	3.26	3.88	20	1035	Ground
0.3048	24.0	1	22.14	527	91	3,856	0.9	0.62	3.26	3.88	50	527	Ground

<sup>a</sup> Abbreviations: “p. air” = passively cooled in air; “a. air” = actively cooled in air; “p. water” = passively cooled in water; “ground” = buried waste form is cooled by conductive heat transfer through earth.

**TABLE A-6 Data for CSLNTM-B-3.0 as function of  $k$  [waste form density = 2.89 g/cm<sup>3</sup>,  $T_g = 527^\circ\text{C}$ , diameter = 0.426 m (16.79 in.)].**

$k$ or $k$ effective [W/(m·K)]	$p$	Centerline Temp. ( $^\circ\text{C}$ )	Surface Temp. ( $^\circ\text{C}$ )
1.10	0.08	476	263
0.96	0.09	501	262
0.86	0.1	526	260
0.55	0.15	644	253
0.40	0.2	751	246
0.31	0.25	843	239
0.25	0.3	921	231
0.75	0	610	274
0.80	0	589	274
0.85	0	571	274
0.90	0	555	274
0.95	0	540	274
1.10	0	505	274
1.20	0	486	274
1.30	0	470	274
1.40	0	456	274
1.50	0	444	274
1.75	0	421	274
2.00	0	403	274





## **Nuclear Engineering Division**

Argonne National Laboratory  
9700 South Cass Avenue, Bldg. 208  
Argonne, IL 60439-4854

**[www.anl.gov](http://www.anl.gov)**



Argonne National Laboratory is a U.S. Department of Energy  
laboratory managed by UChicago Argonne, LLC